Spin Chemical Control of Photoinduced Electron-Transfer Processes in Ruthenium(II)-Trisbipyridine-Based Supramolecular Triads

Thomas Klumpp,[†] **Markus Linsenmann,**[†] **Steven L. Larson,**[‡] **Bradford R. Limoges,**[‡] **Dieter Bürssner,**[†] **Evgenii B. Krissinel,**[†] **C. Michael Elliott,***,[‡] **and Ulrich E. Steiner***,[†]

Contribution from the Fakultät für Chemie, Universität Konstanz, D-78457 Konstanz, Germany, and Department of Chemistry, Colorado State University, Fort Collins, Colorado 80523

Received September 21, 1998. Revised Manuscript Received November 24, 1998

Abstract: Nanosecond time-resolved absorption studies in a magnetic field ranging from zero to 3.0 T have been performed on a series of covalently linked donor−Ru(bipyridine)$_3$−acceptor complexes (D−C^{2+}−A^{2+}). In these complexes the electron donor is a phenothiazine moiety linked to a bipyridine by a $(-CH_2-)_p$ ($p =$ 1, 4, 5, 7) chain, and the electron acceptor is an *N,N′*-diquaternary-2,2′-bipyridinium moiety, linked to a bipyridine by a $(-CH_2-)_2$. chain. On the nanosecond time scale the first detectable photoinduced electron-transfer product after exciting the complex C^{2+} is the charge-separated (CS) state, D$^+$−C^{2+}−A$^+$, where an electron of the phenothiazine moiety, D, has been transferred to the diquat moiety, A^{2+}. In zero field the lifetime of the CS state is about 150 ns. At low fields ($B_0 < 0.5$ T) the magnetic field strongly affects the decay kinetics, splitting it up into a major component, the rate constant of which decreases by a factor of about 10 at fields of several 100 mT, and a minor component with an approximately field independent rate constant. At high fields ($B_0 > 0.5$ T) the total amplitude of the CS absorption signal decreases and the relative contribution of the fast decaying component increases. The magnetic field effects can be consistently interpreted and quantitatively modeled by taking into account the mechanisms and kinetics of the spin multiplicity changes in the CS state and its precursor, a short-lived CT state (D−C^{3+}−A$^+$) formed upon primary electron transfer from the triplet excited complex to the diquat moiety. Exploiting the magnetic field dependent kinetics, the rate constants of the triplet−singlet transitions in the two types of linked radical pairs and of all the electron-transfer processes following the primary one can be assessed. Magnetic-field-dependent investigations thus can be essential for the understanding of the complex kinetics in supramolecular systems with sequential cyclic electron transfer.

Introduction

Photosynthesis provides a natural model upon which to base studies of other light-induced electron-transfer reactions. Investigations of intramolecular charge separation within supramolecular assemblies containing a photoexcitable chromophore (C), an electron acceptor (A), and/or an electron donor (D) have been instrumental in developing a better fundamental, molecular level understanding of the processes by which nature converts solar energy into chemical energy. The literature on such intramolecular photoinduced electron transfers is vast and has been the subject of many recent reviews.[1] While the specifics of individual studies vary, the ultimate long-range goal is to acquire sufficient knowledge to allow chemical systems to be designed and synthesized which can efficiently convert light energy into some other usable form.

An ideal charge-separation system would strongly absorb light over the entire solar spectrum, would have unity quantum efficiency for charge separation, would lose little or none of the incident photon energy, and would yield charge-separated states that did not back electron transfer. Even natural photosynthesis falls short of this ideal, particularly in that considerable incident photon energy is lost in the charge-separation process. In fact, these ideal requirements are highly unrealistic since often the means to attain one goal is the direct opposite of the means to attain another. Nonetheless, the natural photosynthetic reaction center does attain a high quantum efficiency for charge separation without losses from back electron transfer. This has been achieved via an evolutionarily optimized, fixed spatial arrangement of functional molecular components which, through a sequence of fast short-distance electron transfers, separate charge to a large distance and thus avoid the energy-dissipating back electron transfer. This principle of optimized photoinduced charge separation through a series of small distance intramolecular steps (rather than bimolecular reactions or long-distance single-step reactions) has been incorporated into the design of many supramolecular assemblies.[1]

An interesting connection between the study of natural photosynthetic systems and electron-transfer diads and triads can be made. For the natural reaction center, important energetic and kinetic details have been revealed through investigations where the electron-transport chain was artificially blocked either by removing or by pre-reducing the quinone moiety that accepts the electron in the third step.[5] Thereby the function of the natural system is reduced to that of an electron−donor−acceptor triad.

[†] Universität Konstanz.

[‡] Colorado State University.

(1) For a selection of reviews cf. refs 2−4.

(2) *Photoinduced Electron Transfer*; Fox, M. A., Chanon, M., Eds.; Elsevier: Amsterdam, 1988; Vols. A−D.

(3) Photoinduced Electron Transfer I-V. In *Topics in Current Chemistry*; Mattay, J., Ed.; Springer-Verlag: Berlin, 1990−1993; Vols. 156, 158, 159, 163, 168.

(4) Schanze, K. S.; Walters, K. A. Photoinduced electron transfer in metal-organic dyads. In *Molecular and Supramolecular Photochemistry*, Vol. 2: *Organic and Inorganic Photochemistry*; Ramamurthy, V., Schanze, K. S., Eds.; Marcel Dekker: New York, 1998; pp 75−127.

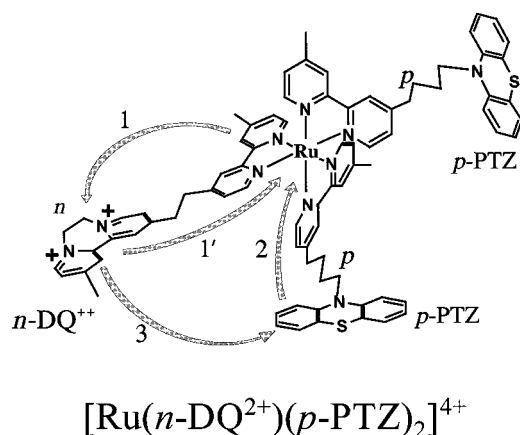(5) Hoff, A. J. *Q. Rev. Biophys.* **1981,** *14*, 599.

$$[\mathrm{Ru}(n\text{-}\mathrm{DQ}^{2+})(p\text{-}\mathrm{PTZ})_2]^{4+}$$

Figure 1. Donor−chromophore−acceptor complex, $\mathrm{Ru}^{II}(n\text{-}\mathrm{DQ}^{2+})(p\text{-}\mathrm{PTZ})_2 = \mathrm{C_{np}}$.

The electron transfer is thus stopped at the stage of the secondary radical ion pair that is amenable to time-resolved optical and EPR investigations. From this modified system the kinetics of back electron transfer, regenerating the chlorophyll special pair in its lowest excited triplet state and ground state, can be studied. In this way, magnetic field and spin effects have turned out to provide much valuable information regarding the details of energetics and structure of the reaction center and its primary photoinduced electron-transfer processes. Likewise, applying spin chemical methods to studies of the kinetics of charge separation and recombination in synthetic supramolecular D−C−A systems can augment the information learned from other time-resolved techniques.

In this work we report spin chemical studies on a series of donor−chromophore−acceptor triads designed in the laboratory of one of the present authors.[7−16] This system of complexes was designed originally to investigate how systematic changes in the energetics and structure of such triads would influence the various rates leading to charge separation and recombination. The goal was to optimize the system for efficient generation of long-lived charge-separated states through manipulation of structure and redox potentials. The complexes involved in the present study (cf. Figure 1) have the general structure [Ru(*p*-PTZ)$_2$(*n*-DQ^{2+})]$^{4+}$ (D−C^{2+}−A^{2+}). The metal complex chromophore has the same redox chemistry and optical spectroscopy as [Ru(DMB)$_3$]$^{2+}$ (where DMB = 4,4′-dimethyl-2,2-bipyridine). As can be seen by the example given in Figure 1, each Ru(L)$_3$ chromophore has appended to it in the 4-position of each bipyridine either an electron donor or acceptor moiety. Two of

the bipyridines are each linked to a phenothiazine donor by a polymethylene chain containing para methylene units (represented as *p*-PTZ). The remaining bipyridine is linked by a two-methylene-unit chain to a diquat electron acceptor. The two quaternary nitrogens of the diquat are linked by a polymethylene chain consisting of *n* methylene units (represented as *n*-DQ^{2+}). The value of *n* determines the redox potential of the diquat and, thus, the driving force for electron transfers involving the DQ^{2+} moiety.

Investigations of (C^{2+}−D)[6] and (C^{2+}−A^{2+})[9−12,14,15] diads and (D−C^{2+}−A^{2+}) triads[7−9,13] with picosecond time-resolved optical spectroscopy have provided evidence of the following processes (cf. Figure 1):

(1) Quenching of the ^{3}MLCT state of the Ru(II) complex by electron transfer to DQ^{2+} generates the CT state Ru^{3+}−DQ$^+$. The time constant of this process, ranging between 250 and 3000 ps, decreases with increasing *n* (decreasing driving force), which is consistent with the process being in the normal Marcus region.[9,12] (1′) Reverse electron transfer regenerates the Ru(II) complex in its ground state. This process is always faster than process 1, so that only a lower limit of ca. (80 ps)$^{-1}$ could be estimated for its rate constant.[9,12] It is important to note that direct detection of the CT state was not possible for either C^{2+}−A^{2+} diads or D−C^{2+}−A^{2+} triads, the reason being that process 2 and the competing process 1′ are both much faster than process 1; consequently, the CS state (D$^+$−C^{2+}−A$^+$) of the triad appears at the same effective rate as the ^{3}MLCT state emission disappears.[9,12] Furthermore, the rates of emission decay are the same between analogous C^{2+}−A^{2+} and D−C^{2+}−A^{2+} complexes, indicating that the initial CT state is D−C^{3+}−A$^+$ irrespective of the presence or absence of donors in the complexes.[7,9,12] Relative changes of the rate constant of process 2 as a function of the number of methylene units in the chain, *p*, have been estimated from the yield of the CS state.[7] For $p \geq$ 4 the effective rate exhibits a moderate monotonic decrease with increasing *p* that can be assigned to the greater average distance between PTZ and Ru. Competing influences of changes in redox potential of PTZ and distance lead to non-systematic *p* dependence for $p < 4$ (cf. ref 17). (3) Finally, the CS state returns to the D−C^{2+}−A^{2+} ground state by electron transfer from DQ$^+$ to PTZ$^+$—a process occurring on the time scale of some 100−300 ns for the whole range of values of *n* and *p* investigated.[13,16]

The present investigation focuses on an aspect that has been completely neglected in the previous investigations of these systems, namely their spin chemistry, i.e. the kinetic role of electron spin processes and the possibility of their modulation by an external magnetic field.[18] This requires explicit consideration of the spin multiplicity of the states involved and application of spin conservation rules in all electron-transfer processes, cf. Scheme 1.

The triplet nature of the photoreactive MLCT state of the Ru complex is well-established.[22] With such a precursor the CT state must be created with initial triplet spin. Therefore

(6) Larson, S. L.; Elliott, C. M.; Kelley, D. F. *Inorg. Chem.* **1996**, *35*, 2070.

(7) Larson, S. L.; Elliott, C. M.; Kelley, D. F. *J. Phys. Chem.* **1995**, *99*, 6530.

(8) Larson, S. L.; Cooley, L. F.; Elliott, C. M.; Kelley, D. F. *J. Am. Chem. Soc.* **1992**, *114*, 9504.

(9) Cooley, L. F.; Larson, S. L.; Elliott, C. M.; Kelley, D. F. *J. Phys. Chem.* **1991**, *95*, 10694.

(10) Ryu, C.; Wang, R.; Schmehl, R.; Ferrere, S.; Ludwikow, M.; Merkert, J.; Headford, C.; Elliott, C. M. *J. Am. Chem. Soc.* **1992**, *114*, 430.

(11) Schmehl, R.; Ryu, C.; Elliott, C. M.; Headford, C.; Ferrere, S. *A.C.S., Adv. Chem. Ser.* **1990**, *211*.

(12) Cooley, L. F.; Headford, C. E. L.; Elliott, C. M.; Kelley, D. F. *J. Am. Chem. Soc.* **1988**, *110*, 6673.

(13) Danielson, E.; Elliott, C. M.; Merkert, J. W.; Meyer, T. J. *J. Am. Chem. Soc.* **1987**, *109*, 2159.

(14) Elliott, C. M.; Freitag, R. A.; Blaney, D. D. *J. Am. Chem. Soc.* **1985**, *107*, 4647.

(15) Elliott, C. M.; Freitag, R. *J. Chem. Soc., Chem. Commun.* **1985**, *156*.

(16) Larson, S. L. Charge transfer in linked donor−chromophore−acceptor systems; Ph.D. Thesis, Colorado State University, 1994.

(17) When $p \leq 3$ the bipyridine attached to the terminal end of the alkyl chain exerts an electronic influence on the PTZ moiety causing a small positive shift in the PTZ$^{0/+}$ potential. For $p > 4$, however, the potential remains effectively invariant (see ref 6).

(18) For reviews see refs 19−21 and references given there.

(19) Salikhov, K. M.; Molin, Y. N.; Sagdeev, R. Z.; Buchachenko, A. L. *Spin Polarization and Magnetic Effects in Radical Reactions*; Elsevier: Amsterdam, 1984.

(20) Steiner, U. E.; Ulrich, T. *Chem. Rev.* **1989**, *89*, 51.

(21) Steiner, U. E.; Wolff, H.-J. Magnetic Field Effects in Photochemistry. In *Photochemistry and Photophysics*; Rabek, J. J., Scott, G. W., Eds.; CRC Press: Boca Raton, 1991; Vol. IV, Chapter 1, pp 1−130.

(22) Demas, J. N.; Taylor, D. G. *Inorg. Chem.* **1979**, *18*, 3177.

reverse electron transfer, 1′, cannot follow immediately but only after spin conversion to singlet. Thus, process 1′ is not an elementary process but it depends on the spin equilibration time $\tau_{s,d}$ and the rate constant of the spin allowed backward transfer, 1′. The spin chemical situation corresponding to processes 1 and 1′ is very similar to that encountered in the quenching of MLCT-excited $Ru(bpy)_3^{2+}$ by methyl viologen, the spin chemistry of which has been well-characterized, both experimentally and theoretically.[23-28] There are two main features specific to this type of spin chemistry: a very fast magnetic-field independent spin relaxation with a characteristic time $\tau_{s,d}$ of $T \rightleftarrows S$ spin equilibration of 20−30 ps[26] (using the notation $\tau_{s,d}$ we emphasize the pecularities of spin relaxation in a strongly spin−orbit coupled coordination compound with d^5 electron configuration as represented by the Ru^{III}-complex species) and a magnetic-field driven $T \leftrightarrow S$ process, caused by the large differences of g factors of the two radicals (Ru^{III}, DQ^+) involved and the strong anisotropy of the **g** tensor of the Ru^{III} complex (as a consequence of this magnetic field effect (MFE) it is expected that the overall efficiency of process 1′ will increase with the magnetic field).

Process 2, wherein an electron is transferred from a doubly occupied molecular orbital of PTZ to the hole in the d^5 configuration of Ru^{III}, is under no spin restriction. It should occur at the same rate for both multiplicities of the CT state (i.e., $k_2 = k_{2'}$). However, the absolute rates of the two processes depend on the populations $[^3CT]$ and $[^1CT]$; thus, since $[^3CT] \gg [^1CT]$, direct population of the ^3CS state will be the significantly more efficient process.

As shown in Scheme 1, the final recombination process regenerating the $D-C^{2+}-A^{2+}$ ground state is spin forbidden from the ^3CS state. Thus spin conversion to ^1CS is necessary and process 3, like process 1′, is a compound process, the overall rate of which is determined by the kinetics of spin equilibration (with effective time constant $\tau_{s,\pi}$) and of the spin-allowed electron-transfer 3. The spin chemical situation of the $^1CS/^3CS$ pair is characteristic of a linked pair of "normal" organic π-radicals which is a classical case of spin chemistry.[19] Here the spin processes are governed by hyperfine coupling, dipolar electron spin−spin coupling, and exchange interaction. An external magnetic field affects the spin equilibration mainly through the Zeeman effect. In general, $T \rightleftarrows S$ processes are retarded with increasing Zeeman level splitting, which generally leads to a slowing down of the rate of $T \rightleftarrows S$ equilibration with increasing magnetic field. However, a finite exchange interaction J expressed in a corresponding S/T splitting may cause T/S level crossing when increasing the field. Such a level crossing becomes apparent as a maximum of the $T \rightleftarrows S$ conversion rate at some field B_{max} characteristic of the value of the exchange splitting.[29,30] Systematic relations between B_{max} and the average separation of radical centers in biradicals have been established.[31-34]

Photoinduced electron transfer in these triad complexes, thus, provides a unique combination of two very different spin chemical situations which are a challenge to explore, especially since such experiments can yield new insights into the details of the electron-transfer processes involved. The triads are available with several variable structural elements. For the present investigation, we took advantage of variations in the length of the methylene bridge linking the pyridine nitrogens,

$$C_{24} = [Ru(2\text{-}DQ^{2+})(4\text{-}PTZ)_2]^{4+}$$

$$C_{34} = [Ru(3\text{-}DQ^{2+})(4\text{-}PTZ)_2]^{4+}$$

$$C_{44} = [Ru(4\text{-}DQ^{2+})(4\text{-}PTZ)_2]^{4+}$$

so as to vary the driving forces of processes 1, 1′, and 3, and to vary the length of the methylene chain linking the phenothiazine donor to the complex while holding the driving force constant,[17] via.

$$C_{41} = [Ru(4\text{-}DQ^{2+})(1\text{-}PTZ)_2]^{4+}$$

$$C_{44} = [Ru(4\text{-}DQ^{2+})(4\text{-}PTZ)_2]^{4+}$$

$$C_{45} = [Ru(4\text{-}DQ^{2+})(5\text{-}PTZ)_2]^{4+}$$

$$C_{47} = [Ru(4\text{-}DQ^{2+})(7\text{-}PTZ)_2]^{4+}$$

Experimental Section

[Ru(p-PTZ)$_2$(n-DQ^{2+})](PF6)$_2$ Complexes. The preparation, purification, and isolation of all of the triad complexes[7,9,12,14] as well as the preparation of the individual p-PTZ and n-DQ^{2+} ligands[6,7,9,12,14] have been reported previously.

Preparation of Samples for Kinetic and Magnetic Field Effect Studies. Solid samples were shipped in a light-tight container under vacuum between the U.S. and Germany. Subsequent to shipping they were stored, protected from light, in a freezer. Solutions for transient spectroscopy studies were typically prepared as follows. A small sample of solid complex was transferred to a 10 mL vial and sufficient spectral quality 1,2-dichloroethane (Fluka) was added to the vial to produce a solution that had an absorbance at 450 nm in a 4 mm path-length cell of between 0.05 and 0.1 (ca. 2.5×10^{-5} M). The solution was immediately transferred to the spectral cell assembly where it was frozen by submersing in liquid N_2. All solution handling to this point was conducted in the dark.

A typical cell assembly consists of an optical measurement chamber that has attached to it a sidearm for freeze−pump−thaw degassing. Cells are sealable under vacuum via a Kontes (or comparable) Teflon/glass valve. The optical portion of the cell consists of a 0.4 cm × 1.0 cm × 4.0 cm rectangular Pyrex compartment that is of standard, not optical, quality (but of entirely sufficient quality for these measurements). Once the solution was transferred into the cell it was tilted to collect all of the liquid in the sidearm where it was frozen. Each sample solution was subjected to a minimum of 3 freeze−pump−thaw cycles to remove any dissolved O_2. After the first of these cycles the solution was no longer protected from room light in routine handling. However, when not in use the solutions in the cells were stored under vacuum in the freezer protected from light. Generally, the sample solutions after

(23) Steiner, U. E.; Wolff, H.-J.; Ulrich, T.; Ohno, T. *J. Phys. Chem.* **1989**, *93*, 5147.

(24) Steiner, U. E.; Bürssner, D. *Z. Phys. Chem. N.F.* **1990**, *169*, 159.

(25) Wolff, H.-J.; Steiner, U. E. *Z. Phys. Chem. N.F.* **1990**, *169*, 147.

(26) Bürssner, D.; Wolff, H.-J.; Steiner, U. E. *Z. Phys. Chem. N. F.* **1993**, *182*, 297.

(27) Bürssner, D.; Wolff, H.-J.; Steiner, U. E. *Angew. Chem. Int. Ed.* **1994**, *33*, 1772.

(28) Wolff, H.-J.; Bürssner, D.; Steiner, U. E. *Pure Appl. Chem.* **1995**, *67*, 167.

(29) Sakaguchi, Y.; Hayashi, H.; Nagakura, S. *Bull. Chem. Soc. Jpn.* **1980**, *53*, 39.

(30) Staerk, H.; Treichel, R.; Weller, A. Polymethylene-Linked Radical Ion Pairs in Magnetic Fields. In *Biophysical Effects of Steady Fields, Springer Proceedings in Physics*; Maret, G., Kiepenheuer, J., Boccara, N., Eds.; Springer-Verlag: Berlin, 1986, Vol. 11, pp 85−89.

(31) Weller, A.; Staerk, H.; Treichel, R. *J. Chem. Soc., Faraday Discuss.* **1984**, *78*, 271, 332.

(32) Weller, A. Chain effect and magnetic field effect on the photoinduced electron transfer reactions of polymethylene-linked donor acceptor systems. In *Supramolecular Photochemistry*; Balzani, V., Ed.; D. Reidel Publishing Company: Dordrecht, The Netherlands, 1987; pp 343−354.

(33) Bittl, R.; Schulten, K. *Chem. Phys. Lett.* **1988**, *146* (1,2), 58.

(34) Closs, G. L.; Forbes, M. D. E.; Piotrowiak, P. *J. Am. Chem. Soc.* **1992**, *114*, 3285.

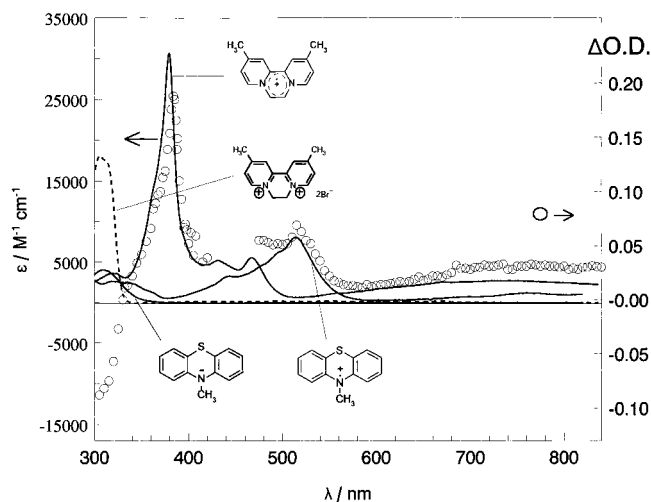(35) Ulrich, T.; Steiner, U. E.; Schlenker, W. *Tetrahedron* **1986**, *42*, 6131.

Figure 2. (○) Transient absorption spectrum recorded at its maximum during the laser pulse for complex C_{24} in 1,2-dichloroethane. Also shown are the absorption spectra of individual components DQ^{2+}, DQ^{1+},[36] and *N*-methylphenothiazine and its cation radical.[72]

careful degassing showed no visible spectral changes over the course of several weeks. Changes in the spectrum were indications of O_2 leaks.

Nanosecond laser flash photolysis experiments were carried out on the dye-laser system described in refs 25 and 35, however with a Nd-YAG laser (Quanta Ray GCR 150-5) operated at its third harmonics (355 nm) as a pump laser.[36] The laser pulse width was 5−7 ns. Coumarin 47 (Radiant Dyes) in methanol was used in the dye laser, which was operated at 460 nm. The pulse energy was adjusted to about 3 mJ, exciting the sample over a cross section of about 5 mm². The laser was run at a repetition rate of 1 Hz and the transient signals were averaged over typically 32 pulses. The optical path through the cell was along the 1.0 cm dimension. The cell was placed between the pole pieces of a Bruker B-E 15 electromagnet. The magnetic field was applied perpendicular to the optical path along the 0.4 cm dimension. The magnetic induction was measured by a Hall probe (Bell, STB1-0404). For experiments at zero field care was taken to compensate the remanent field of the pole pieces by reversing the current through the magnet.

Results

From previous picosecond time-resolved studies[7,8] it is known that the decay time of the luminescent MLCT state of the complexes increases in the series C_{24}, C_{34}, C_{44} ($\tau_{MLCT} = 0.24$, 0.96, 3.12 ns) in correspondence with the decreasing reduction potential of the diquat moiety ($E_{DQ++/DQ+} = -0.43$, -0.64, -0.77 V vs SCE). Accordingly, given the 6 ns fwhm pulse width of the laser, in our experiments noticeable concentrations of the MLCT state are detected during the laser pulse only for complexes C_{41}, C_{44}, C_{45}, and C_{47} which share the same 4-DQ^{2+} moiety. Several nanoseconds after the laser pulse the transient spectra observed for all the triads investigated here exhibit the same characteristic features as displayed for compound C_{24} in Figure 2.

Spectra of relevant individual components absorbing in the scanned spectral region are also shown in Figure 2. From these spectra it is evident that the observed transient spectrum indicates the disappearance of DQ^{2+} by a bleaching in the spectral region of the DQ^{2+} absorption and formation of the radical ions DQ^+ and PTZ^+ since the positive changes of optical density correspond to an equimolar superposition of the two
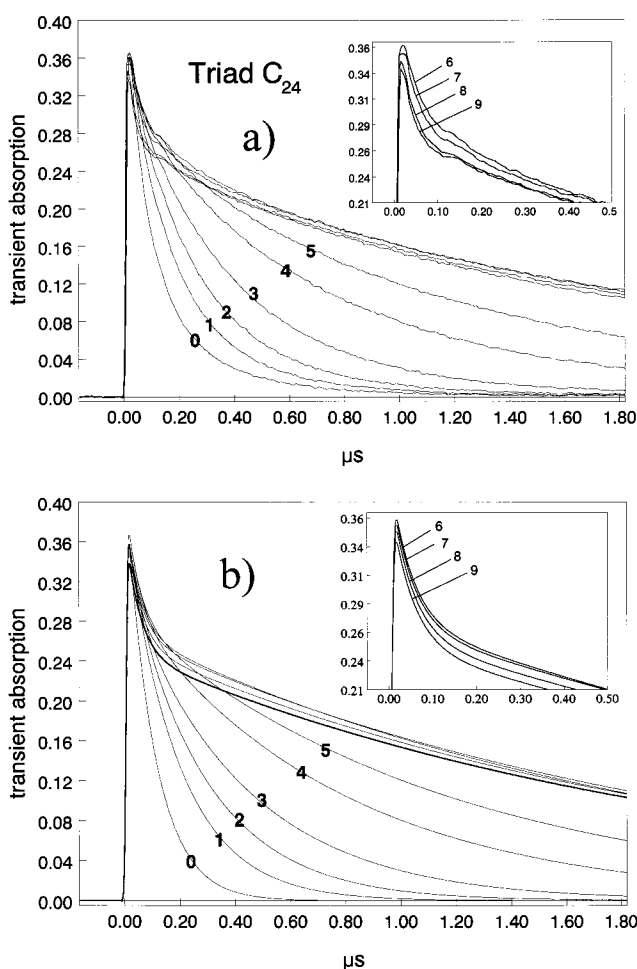
(36) Linsenmann, M. Spinchemische Untersuchung des Zusammenhangs zwischen thermodynamischer Triebkraft und Geschwindigkeit von Elektronentransferprozessen in frei diffundierenden Radikalionenpaaren; Dissertation: Universität Konstanz, 1997.
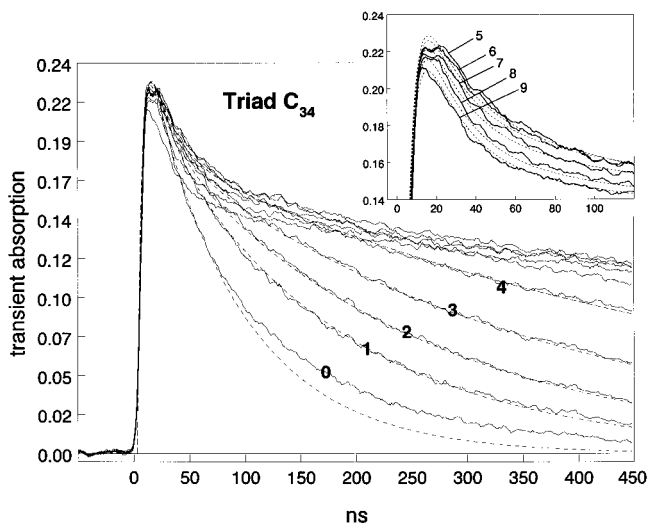

Figure 3. (a) Decay of transient absorption of the CS state ($\lambda_{obs} = 390$ nm) for triad C_{24} in different magnetic fields: (0) 0 T, (1) 5 mT, (2) 10 mT, (3) 20 mT, (4) 50 mT, (5) 100 mT, (6) 500 mT, (7) 1000 mT, (8) 2000 mT, and (9) 3000 mT. The inset shows an enlargement of the initial stage for curves 6−9. (b) Simulations, cf. text.

radical absorptions. Thus there is conclusive evidence of fast formation of the CS state within at most a few nanoseconds.[37]

Typical decay profiles of the CS state and its magnetic field dependence are shown for triads C_{24}, C_{34}, and C_{41} in Figures 3−5. In zero magnetic field the decays for all of the triad complexes studied are close to monoexponential with decay times between 100 and 200 ns (cf. Table 1). As the magnetic field increases, the decays become distinctly biexponential; the major component slows down considerably, but the rate constant of the fast (minor) component remains approximately constant. The field dependence of the slower component is strictly monotonic and tends toward a saturation limit at about 0.5 T. The pertinent zero-field and high-field values are listed in Table 1. It is noteworthy that for most of the triads the lifetime of the major part of the CS state is increased by as much as a factor of 7−12 in moderate magnetic fields. Only triad C_{41} is exceptional in this respect. Here the lifetime of the major component increases only by a factor of 2.5.

(37) Comparing the transient spectrum for the CS state of C_{24} shown in Figure 2 with that of C_{34} published in ref 13, one notes that the intensity ratio of the absorption maxima at 390 and 520 nm exhibits a significant difference (1.17 for C_{24} and 2.75 for C_{34}). This is due to the strong effect that the length of the $-(CH_2)_n-$ bridge in the diquat moiety has on the twist of the two aromatic rings and hence on the absorption intensities. The transient spectra observed are in qualitative accord with spectroelectrochemical measurements[36] yielding extinction coefficient maxima for the $DQ^{+\bullet}$ moiety in water of $\epsilon_{379} = 30500$ M^{-1} cm^{-1} and $\epsilon_{385} = 13900$ M^{-1} cm^{-1} for 2-$DQ^{+\bullet}$ and 3-$DQ^{+\bullet}$, respectively.

Figure 4. (a) Decay of transient absorption of the CS state ($\lambda_{obs} = 390$ nm) for triad C_{34} in different magnetic fields: (0) 0 T, (1) 5 mT, (2) 10 mT, (3) 20 mT, (4) 50 mT, (5) 100 mT, (6) 500 mT, (7) 1000 mT, (8) 2000 mT, and (9) 3000 mT. The inset shows an enlargement of the initial stage for curves 5−9. The dashed lines represent theoretical simulations of the respective curves.

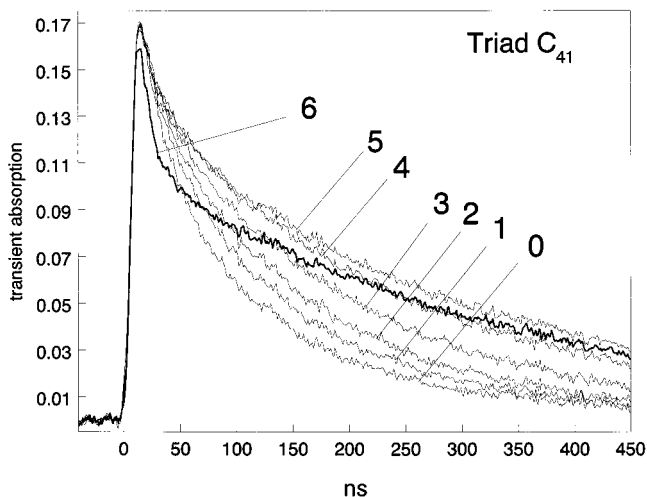**Figure 5.** Decay of transient absorption of the CS state ($\lambda_{obs} = 385$ nm) for triad C_{41} in different magnetic fields: Light lines, from below, 0, 5, 10, 20, 50, 100, 500, 1000, 2000, mT; heavy line, 3000 mT.

Table 1. Rate Constant of Slow Component k_a of CS-State Decay in Zero Field and at 0.5 T. For the Definition of k_a cf. Eqs 4 and 5

triad	$k_a(0\ \text{T})$,[a] s^{-1}	$k_a(0.5\ \text{T})$, s^{-1}
C_{24}	8.7×10^6	0.5×10^6
C_{34}	11.9×10^6	1.0×10^6
C_{44}	10.6×10^6	0.8×10^6
C_{41}	9.4×10^6	3.8×10^6
C_{45}	5.3×10^6	0.8×10^6
C_{47}	7.7×10^6	1.0×10^6

[a] Most of the zero-field curves exhibit an additional decay tail.

Fields higher than 0.5 T have little further effect on the time constants of the two decay components, but they do affect their amplitudes. A decrease of the overall (initial) signal amplitude becomes noticeable at a field of 1 T and continues to an overall reduction in signal intensity between 5 and 10% at 3 T, the highest field applied. It must be pointed out, though, that this amplitude effect is not saturated at this field. Another high-field feature is clearly demonstrated in the curves displayed in Figures 3−5. Comparing the values at their maxima and

Scheme 1
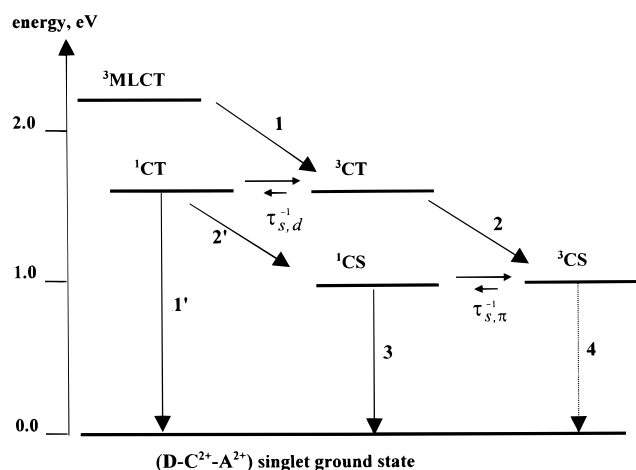
at the point where the slow component has first become predominant (i.e., about 150 ns after the maximum) there is a more pronounced magnetic-field-induced decrease in the signal intensity at the latter point. This behavior is indicative of an increase in the relative amplitude of the fast component with a concomitant decrease in the amplitude of the slow component.

Discussion

As to be expected from the earlier picosecond time-resolved experiments,[7,8] the present nanosecond time-resolved investigations did not provide direct spectroscopic evidence for species other than the emissive ^{3}MLCT state and the final CS state. The kinetics of the CS state, however, shows diverse MFEs which reveal mechanistic details of the recombination process from which quite detailed conclusions can be drawn about the nature and behavior of the intervening CT state. The MFEs apparent in the kinetic profiles measured for the CS state may be characterized as follows: (i) in the low-field region ($0 < B_0 < 0.5$ T) the time profile of the decay kinetics undergoes a drastic change and (ii) in the high-field region ($B_0 > 0.5$ T) the time constant of the fast component of the decay is rather invariant; however, (a) the amplitude of the CS signal and (b) the relative contributions of the fast and slow components vary, and this variation is not saturated up to 3 T, the highest field applied.

We will now discuss and analyze in detail the mechanisms and processes underlying these MFEs. Since the radical pair (RP) character of both the CS and the CT state will be essential to this end, in the following we will designate these states as CS-RP and CT-RP states, respectively, to emphasize this aspect.

(i) The Low-Field Effect. The characteristics of the low-field effect are, again, illustrated by the signal traces in Figures 3−5. While Figures 3 and 4 for complexes C_{24} and C_{34} are representative of the majority of the complexes investigated, complex C_{41} (Figure 5) with the shortest link ($p = 1$) between PTZ moiety and the bipyridine is clearly distinct from the others and will be discussed separately.

What is characteristic of the majority of cases (cf. Figures 3 and 4) is the drastic slowing of the CS recombination kinetics with increasing magnetic field and the development of very marked biexponential decay kinetics with the faster component keeping a relatively constant decay rate. Except for triad C_{41} the rate constant of the slower part of the CS-RP decay decreases by about a factor of 10 between zero field and 0.5 T. Such enormous lifetime increases have been seen with some other

Scheme 2
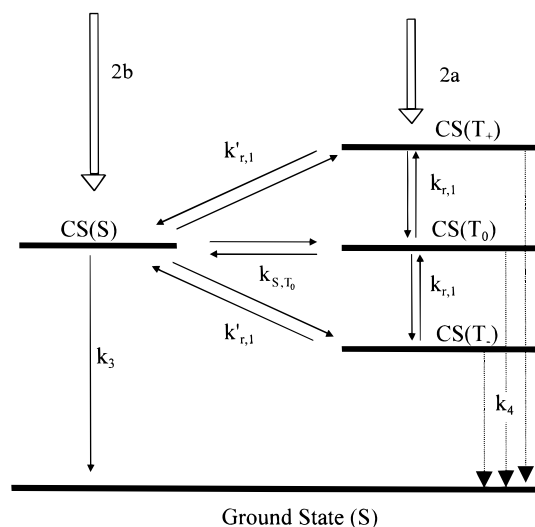
biradical systems,[38] but they are of practical interest for the present systems which were originally devised to mimic essential photosynthetic functions of photoinduced charge separation. In general, the magnetic field dependent decrease of the recombination rate of a radical pair to a diamagnetic product is an indication of the radical pair being created with *triplet* spin correlation. Examples of such MFEs are numerous in the literature and are typically observed for radical pairs which cannot separate after formation either because they are trapped in micellar supercages[43-48] or they are chemically linked by some flexible spacer.[38] However, what has not been observed previously in such a clear way is the breaking up of the kinetics into two very different kinetic stages (although it has been predicted from theoretical models of the radical pair mechanism).[49,50] To analyze the magnetic field dependence of the CS recombination kinetics quantitatively we apply a kinetic model shown in Scheme 2. It is a generalization[53,54] of the scheme put forth by Hayashi and Nagakura[49] in accounting for MFEs according to the so-called *relaxation mechanism*.

(38) For a selection of examples, see refs 34 and 39−42.
(39) Doubleday, C., Jr.; Turro, N. J.; Wang, J.-F. *Acc. Chem. Res.* **1989**, *22*, 199.
(40) Johnston, L. J.; Scaiano, J. C. *Chem. Rev.* **1989**, *89*, 521.
(41) Wang, J.; Doubleday, C., Jr.; Turro, N. J. *J. Phys. Chem.* **1989**, *93*, 4780.
(42) Tanimoto, Y.; Takashima, M.; Hasegawa, K.; Itoh, M. *Chem. Phys. Lett.* **1987**, *137*, 330.
(43) Sakaguchi, Y.; Hayashi, H. *Chem. Phys. Lett.* **1982**, *87*, 539.
(44) Ulrich, T.; Steiner, U. E. *Chem. Phys. Lett.* **1984**, *112*, 365.
(45) Turro, N. J.; Zimmt, M. B.; Gould, I. R. *J. Phys. Chem.* **1988**, *92*, 433.
(46) Gould, I. R.; Zimmt, M. B.; Turro, N. J.; Baretz, B. H.; Lehr, G. F. *J. Am. Chem. Soc.* **1985**, *107*, 4607.
(47) Evans, C.; Ingold, K. U.; Scaiano, J. C. *J. Phys. Chem.* **1988**, *92*, 1257.
(48) Levin, P. P.; Kuzmin, V. A. *Dokl. Phys. Chem.* **1987**, 26.
(49) Hayashi, H.; Nagakura, S. *Bull. Chem. Soc. Jpn.* **1984**, *57*, 322.
(50) The absence of a clearly appearing biexponentiality in the decay of biradicals has puzzled the authors of ref 41 and has been tentatively explained by suggesting unusually strong initial triplet polarization. In other systems[52] potential reasons may lie in slow formation rates of triplet RPs in bimolecular reactions. Under such conditions the fast part of the RP decay could be obscured by the delay of the RP formation.
(51) Wang, J.; Doubleday, C., Jr.; Turro, N. J. *J. Phys. Chem.* **1989**, *93*, 4780.
(52) Sakaguchi, Y.; Hayashi, H. *J. Phys. Chem.* **1984**, *88*, 1437.
(53) Steiner, U. E.; Wu, J. Q. Unpublished.
(54) Wu, J. Q. Spin relaxation mechanisms controlling magnetic-field dependent radical pair recombination kinetics in nanoscopic reactors. Ph.D. Dissertation: Universität Konstanz, 1993.

Since recombination of the CS-RP can only lead to the diamagnetic singlet ground state, the spin conservation rule (cf. ref 20) demands that the unpaired spins in the CS-RP be singlet correlated for the pair to be reactive. The rate constant of such spin-allowed recombination is denoted k_3. Recombination to the singlet ground state should be spin forbidden for CS-RPs with triplet spin correlation. However, it has been noted that the spin conservation rule can be relaxed in spin−orbit active biradicals and RPs[55-57] so that, in particular with regard to the heavy atom nature of the sulfur center in the PTZ$^{+\bullet}$ radical, the possibility of direct recombination of ^{3}CS-RPs should be explicitly taken into account although the corresponding rate constant k_4 should be much smaller than k_3. It should be pointed out that spin−orbit assisted recombination of ^{3}CS-RPs should be kinetically distinguished from spin−orbit based spin relaxation interconverting ^{3}CS and ^{1}CS. For a detailed study that distinguishes between these two alternatives cf. ref 55. Furthermore, it is important to note that the rates of such spin−orbit assisted chemical processes are not magnetic field dependent in low or moderate magnetic fields. Even though the spin conservation rule may not be absolutely strict, from the fact that $k_3 \gg k_4$ it follows that if the CS-RP is created with an initial triplet spin (process 2a in Scheme 2) a spin conversion to singlet will open up a much faster channel for recombination. On the other hand, if the CS-RP is generated with an initial singlet spin (process 2b in Scheme 2), spin conversion processes can compete with the recombination process (k_3) and slow down the overall decay of the CS state. Hence explicit kinetic accounting for the spin processes is necessary to understand the observed kinetics and its magnetic field dependence.

In general, the electron spin in a radical pair can be affected by coherent and by incoherent processes. In organic RPs with only weak spin−orbit coupling the coherent processes are mainly driven by isotropic hyperfine couplings which—since they are local interactions in the individual radicals—tend to *decouple* the electron spins of the pair or, in equivalent terms, *mix* S and T states of the radical pair. However, such effects can only occur if the energy difference between the states to be mixed does not significantly exceed the strength of the hyperfine coupling. Therefore an external magnetic field of a suitable strength will make such mixings between the outer Zeeman components, $T_{\pm}$, and the S (and T_0) component inefficient, while not affecting the T_0−S mixing. The time scale on which coherent hyperfine-induced spin state mixing occurs can be estimated by using the semiclassical effective hyperfine field $B_{1/2}$ defined as[21,58]

$$B_{1/2} = \left(3\sum_i a_i^2 I_i(I_i + 1)\right)^{1/2} \tag{1}$$

where a_i and I_i are the isotropic hyperfine coupling constant and nuclear spin quantum number of a nucleus and the index i runs over all magnetic nuclei of the RP.

For the PTZ$^{+\bullet}$··DQ$^{+\bullet}$ radical pair the hyperfine coupling constants published in ref 59 for PTZ$^{+\bullet}$ ($1 \times a_N = 0.63$ mT, $1 \times a_H = 0.73$ mT, $2 \times a_H = 0.25$ mT, $2 \times a_H = 0.11$ mT, $2 \times a_H = 0.05$ mT) and in ref 60 for n-DQ$^{+\bullet}$ ($n = 2$) ($2 \times a_N = 0.4$ mT, $4 \times a_H = 0.35$ mT, $2 \times a_H = 0.31$ mT, $2 \times a_H = 0.25$

(55) Wu, J. Q.; Baumann, D.; Steiner, U. E. *Mol. Phys.* **1995**, *84*, 981.
(56) Khudyakov, I. V.; Serebrennikov, Y. A.; Turro, N. J. *Chem. Rev.* **1993**, *93*, 537.
(57) Levin, P. P.; Kuzmin, V. A. *Chem. Phys. Lett.* **1990**, *165*, 302.
(58) Weller, A.; Nolting, F.; Staerk, H. *Chem. Phys. Lett.* **1983**, *96*, 24.
(59) Depew, M. C.; Zhongle, L.; Wan, J. K. S. *J. Am. Chem. Soc.* **1983**, *105*, 2480.
(60) Rieger, A. L.; Rieger, P. H. *J. Phys. Chem.* **1984**, *88*, 5845.

mT, $2 \times a_H = 0.06$ mT, $2 \times a_H = 0.03$ mT) yield a value of $B_{1/2} = 2.82$ mT, which when converted into a Larmor frequency corresponds to an effective rate constant of about $k_{coh} = 5 \times 10^8$ s^{-1} for degenerate S/T mixing. If the ^{1}CS-RP recombination rate constant k_3 is clearly smaller than that value, S/T spin equilibrium will be established prior to recombination. Whereas this condition may be fulfilled in zero field, it will possibly be invalid for T_+ and T_- at magnetic field values $B_0 > B_{1/2}$, where spin conversion to S and T_0 may become much slower than k_3 and hence will become rate determining for the recombination of the $T_\pm$ population of the CS-RP.

Whether this will indeed be the case depends on the magnetic field dependence of *incoherent* processes converting $T_\pm$ to T_0 and S, i.e. longitudinal spin relaxation. Mechanistically these processes are due to stochastic modulations of the electron spin Hamiltonian due to (1) anisotropic hyperfine coupling (*ahf* mechanism), (2) **g**-tensor anisotropy (*gta* mechanism), (3) spin-rotational coupling (*src* mechanism), and (4) electron spin−spin dipolar interaction (*esdi* mechanism). At low fields mechanisms (1) and (4) dominate. They should follow a Lorentzian field dependence:[21,61]

$$k_{1,r} + k'_{1,r} = \frac{2}{\hbar^2}\overline{V^2}\frac{2\tau_c}{1 + \omega_0^2\tau_c^2} \qquad (2)$$

where $\overline{V^2}$ is the mean square value of a fluctuating coupling matrix element, τ_c is the correlation time of this process, and ω_0 is the angular frequency corresponding to the energy splitting of the two levels involved which increases linearly with the magnetic field. Since for mechanisms 1 and 4 the coupling matrix element is independent of the external magnetic field, $k_{1,r} + k'_{1,r}$ will be constant at low fields and decrease as B_0^{-2} at fields where $\omega_0^2\tau_c^2 > 1$. For typical situations the relevant correlation times of mechanisms 1 and 4 are between 10^{-10} and 10^{-9} s so that the turnover point of the field dependence is in the region of several mT.

In general, mechanisms 2 and 3 are also described in the framework leading to expression 2. However, for the *gta* mechanism $\overline{V^2} \propto B_0^2 \propto \omega_0^2$ leading to a field dependence reciprocal to that of mechanisms 1 and 4, i.e. increasing with B_0^2 at low fields and reaching a saturation value at high fields. For the *src*-mechanism 4 the correlation time is so short[62] that the turnover from B_0 independence to B_0^2 dependence is usually not reached at normally available laboratory fields. Estimations of $k_{1,r} + k'_{1,r}$ values for the *gta* and *src* mechanism, both of which can be related to **g**-tensor deviations from the value of the free electron, have been given for the selenine radical that exhibits stronger spin−orbit coupling ($g = 2.0083$ (cf. ref 55)) than the PTZ$^{+\bullet}$ radical ($g = 2.0052$, (cf. ref 60)). From the results derived in ref 55 one may conclude that neither the *src* nor the *gta* mechanism will lead to $k_{1,r} + k'_{1,r}$ values larger than 10^5 s^{-1} which, as to be shown below, is kinetically negligible in relation to k_4 in the present systems.

The scenario outlined above is essentially the "relaxation mechanism" as it was explicitly introduced into spin chemistry by Hayashi and Nagakura.[49] In the following we will give its kinetic results for the generalized case[53,54] of simultaneous population of the RP's S and T states to variable degrees (s and $1 - s$, respectively) and for possible recombination of the S-RP (k_3) *and* the T-RP (k_4). It is assumed that $k_{S,T_0} \gg k_3$ so that the $^3CS(T_0) \rightleftharpoons {}^1CS$ equilibrium is maintained throughout

(61) Lüders, K.; Salikhov, K. M. *Chem. Phys.* **1987**, *117*, 113.
(62) Atkins, P. W.; Kivelson, D. *J. Chem. Phys.* **1966**, *44*, 169.

the lifetime of the CS-RP. In general, the longitudinal relaxation rate constants connecting $T_\pm$ with S ($k'_{r,1}$) and $T_\pm$ with T_0 ($k_{r,1}$) must be distinguished, but as it turns out, the observable RP kinetics depends only on the sum $k'_{r,1} + k_{r,1}$ which will be denoted as k_r.

For a general value of s, the absorption signal $A(t)$ of the CS state is given by:

$$A(t) = A_0 \cdot \{(1 - s)[CS]_T(t) + s \cdot [CS]_S(t)\} \qquad (3)$$

$[CS]_T$ and $[CS]_S$ are the CS-state population functions for pure T-population ($s = 0$) or pure S-population ($s = 1$), respectively. Their time dependence is given by:

$$[CS]_T(t) = c_{T,a} \cdot e^{-k_a \cdot t} + c_{T,b} \cdot e^{-k_b \cdot t} \quad (\text{at } t > 0) \qquad (4)$$

$$[CS]_S(t) = c_{S,a} \cdot e^{-k_a \cdot t} + c_{S,b} \cdot e^{-k_b \cdot t} \quad (\text{at } t > 0) \qquad (5)$$

with the definitions

$$c_{T,a} = \frac{1}{2} + \frac{3k_r + (k_3 - k_4)/4}{6\Delta}, \quad c_{T,b} = \frac{1}{2} - \frac{3k_r + (k_3 - k_4)/4}{6\Delta} \qquad (6a,b)$$

$$c_{S,a} = \frac{1}{2} + \frac{k_r - (k_3 - k_4)/4}{2\Delta}, \quad c_{S,b} = \frac{1}{2} - \frac{k_r - (k_3 - k_4)/4}{2\Delta} \qquad (7a,b)$$

$$k_a = k_r + \frac{1}{4}k_3 + \frac{3}{4}k_4 - \Delta, \quad k_b = k_r + \frac{1}{4}k_3 + \frac{3}{4}k_4 + \Delta \qquad (8a,b)$$

$$\Delta = \sqrt{k_r^2 + (k_3 - k_4)^2/16} \qquad (9)$$

Since the magnetic field shifts the value of k_r in a wide range from $k_r \gg k_3 \gg k_4$ to $k_3 \gg k_4 \gg k_r$ it is instructive to note the analytical results for the two observed rate constants k_a and k_b in these limiting cases:

(a) For the zero-field case where $k_r \gg k_3 \gg k_4$ applies, one obtains a degeneration of the biexponential decay into a monoexponential one ($c_{T,b} = c_{S,b} = 0$) with

$$k_a = \frac{1}{4}k_3 + \frac{3}{4}k_4 \qquad (10)$$

(b) For the high-field case where $k_3 \gg k_4 \gg k_r$ applies, the fast rate constant will approach a limiting value of

$$k_b = \frac{1}{2}k_3 + \frac{1}{2}k_4 \qquad (11)$$

whereas the slow one reaches a value of

$$k_a = k_4 \qquad (12)$$

The amplitudes of these kinetic components depend on the initial spin character of the RP. For an initially pure triplet, one has

$$c_{T,a} = \frac{2}{3}, \quad c_{T,b} = \frac{1}{3}$$

For an initially pure singlet, one has

$$c_{S,a} = 1, \quad c_{S,b} = 0$$

According to this formalism there are five parameters A_0, s, k_3, k_4, and k_r to fit the decay of the CS transient signals. This seems to introduce a lot of ambiguity, but there are indeed sufficient and independent criteria to determine these values uniquely. First

Table 2. Parameters for the Theoretical Curves Shown in Figure 5b for C_{34}[a]

curve no.	magn. field, mT	A_0	s	k_r, s^{-1}
0	0	0.270	0.00	1.7×10^7
1	5	0.270	0.00	6.0×10^6
2	10	0.270	0.00	3.9×10^6
3	20	0.270	0.00	2.3×10^6
4	50	0.270	0.00	1.1×10^6
5	100	0.270	0.00	6.8×10^5
6	500	0.268	0.02	2.8×10^5
7	1000	0.265	0.05	1.8×10^5
8	2000	0.260	0.09	0.3×10^5
9	3000	0.253	0.09	0.0×10^5

[a] The values for k_3 (9×10^7 s^{-1}) and k_4 (7.2×10^5 s^{-1}) were the same for all curves. For the variation in parameter values for A_0 and s tolerated by the fit see Figure 9.

of all, the two observable decay constants k_a and k_b are solely determined by the rate parameters k_3, k_4, and k_r. Second, since k_3 and k_4 are magnetic field independent they must be considered as "global" parameters for a complete set of magnetic field dependent curves. To reproduce the magnetic field dependence of the observed kinetic curves for each compound, there is actually only one free parameter, namely the relaxation rate constant k_r.

The signal amplitude is determined by A_0, which is a relative measure of the yield of CS-RPs produced. Determination of this quantity is independent of all the others. The parameter s, specifying the initial singlet character with which the CS state is formed, determines the ratio of the fast and slow components in the decay. Of course, the pertinent results and their possible magnetic field dependences must be subject to a plausible mechanistic rationalization.

A detailed kinetic fit including the earliest steps of the CS kinetics was only feasible for complexes C_{24} and C_{34} because only here was the reaction of the ^{3}MLCT state clearly shorter than the laser width so that the initial CS absorption was not obscured by signal components due to ^{3}MLCT. In Figures 3 and 4 we show the fit curves according to the described procedure. To reproduce the initial "round off" of the signal, the response time of the equipment was taken into account by analytically convoluting the ideal kinetic response according to eqs 4 and 5 with an exponential decay function equivalent to 4 ns response time.

For complex C_{34}, where the measurements were done with optimum time resolution and highest accuracy, the strategy and accuracy of the kinetic fit procedure shall be described in some detail. Actually, to fix k_3 and k_4 the high-field curves are best suited. For the highest field k_r can be assumed to be negligible so that k_4 is determined from the slowly decaying part and $^1/_2$-($k_3 + k_4$) from the fast part. The values thus determined for k_3 and k_4 are then kept fixed throughout the set of curves and only k_r is adjusted as a kinetic parameter, apart from the amplitude quantities A_0 and s. The complete set of fit parameters is listed in Table 2. As can be seen in Figure 4, the fit to the experimental signals is very good except for the very first curve in zero field, the tail of which cannot be fully accommodated within the rigid kinetic criteria just described. For complex C_{24} the corresponding results, though somewhat more scattered, indicate the same behavior: very small s and magnetic-field independence of A_0 and s in the low-field regime.

The s values characterizing the fits of the CS-RP decays for all the triads investigated amount to less than 10%, which is conclusive evidence that the CS-RPs originate with almost pure triplet multiplicity. This of course reflects the spin memory of the primary photoreactive ^{3}MLCT state of the Ru complex and

demonstrates that this spin memory is well-preserved during the life span of the intermediate CT state. As the magnetic field exceeds 0.5−1.0 T the initial singlet character of the CS-RP increases noticeably, a change that parallels a slight decrease of the amplitude factor A_0. The origin of the latter effects will be discussed below.

Except for triad C_{41} the values obtained for k_3, the spin-allowed recombination rate constant of the CS-RP, are in the range $(0.6−1) \times 10^8$ s^{-1} while the values of k_4 are about 100 times smaller than k_3. In seeking an appropriate framework of interpretation of these values one should be aware of the fact that the spacers by which the DQ^{2+} and the PTZ moieties are fixed to the central complex are rather flexible and allow for the corresponding radicals to change their relative positions and distance in a wide range from encounter distance, where the local rate constant of electron transfer according to the exergonicity of the recombination reaction should be much faster than the observed effective value of k_3, up to quite extended conformations where the rate constant for remote electron transfer will be significantly slower.

Regarding the structure of the triads investigated here one has to note that a number of different isomers result from the relative orientations of the three bpy ligands, each of which is unsymmetrically linked to a n-DQ^{2+} or PTZ moiety. Concerning the possible approaches between $DQ^{+\bullet}$ and $PTZ^{+\bullet}$ radicals one has to distinguish isomers where $PTZ^{+\bullet}$ is "cis" to $DQ^{+\bullet}$ and one where it is "trans". In the latter, less probable case, direct encounters of $DQ^{+\bullet}$ and $PTZ^{+\bullet}$ through suitable conformations of the spacer chains are sterically extremely unlikely. Therefore it is expected that recombination of CS-RPs in triads with *trans* configuration is slower than that in *cis* isomers. Except for direct electron transfer in such unfavorable conformations where they manage to come close enough, other pathways of electron transfer that might contribute here involve superexchange mediated electron transfer through the intervening bpy ligands, or indirect, sequential electron transfer through degenerate electron exchange between $PTZ^{+\bullet}$ and PTZ in the same triad whereupon trans isomers are converted to cis isomers. For cis isomers which statistically should make up for 75% of the whole ensemble, the $DQ^{+\bullet}$−$PTZ^{+\bullet}$ distance for $p = 4$ is ca. 15 Å if the spacers are extended into a direction pointing radially away from the center (cf. Figure 1). This may be considered a situation with average separation between $DQ^{+\bullet}$ and $PTZ^{+\bullet}$ which is lengthened and shortened according to the chain dynamics of the spacers. Even for the average separation, electron transfer is probably slower than the effective rate constants k_3 determined here. This means that the electron-transfer rate is probably controlled by the encounter rate of the two radical pendants. In that sense the situation is quite comparable to unlinked RPs trapped in micellar super cages: for RPs in water nanodroplets of reversed micro emulsions[63] it has been shown that the rate of recombination is "diffusion controlled" in that it varies with the inverse power of the volume of the nanodroplets. For example, for a RP composed of a semireduced thionine radical and an aniline cation radical in an aqueous nanocage of 25 Å radius, the recombination rate constant of the S-RP is about 10^7 s^{-1} which is ca. 10 times slower than observed for the CS-RPs in our triads. On the other hand, the k_4 value in the same microheterogeneous system is 2.5×10^6 s^{-1}, i.e., 4 times faster than that for the CS-RPs in the triads. The greater similarity of spin-allowed and spin-forbidden rate constants in the micellar case may be due to more favorable conditions for intermolecular

(63) Ulrich, T.; Steiner, U. E. *Chem. Phys. Lett.* **1984**, *112*, 365.
(64) Kanter, F. J. J. de; Hollander, J. A. den; Huizer, A. H.; Kaptein, R. *Mol. Phys.* **1977**, *34*, 857.

spin−orbit coupling effects in the unlinked system which has more freedom to adjust optimum overlap for spin-inverted electron transfer to occur and to a higher microviscosity, extending the contact time of RPs and thereby supporting the ISC process. Altogether it seems that the k_3 and k_4 values determined for the triad CS-RPs are reasonably well explained.

A final comment must be given, however, to account for the deficiency of the kinetic model in case of the zero-field curve (cf. Figure 4). We suggest that the extended tail of the decay in this case reflects the distribution of k_3 values due to different isomers. In a magnetic field where k_r is decreased, the slow part of the decay kinetics is dominated by the sum of the rate constants $k_r + k_4$ and the inhomogeneity of k_3 may be obscured. Of course there also should be a difference in k_4 values of the two isomers. However, on the time scale where k_4 dominates the kinetics, the degenerate electron-transfer equilibrium between the two isomers is probably established so that one single value of k_4 appears which corresponds to the statistical average of the k_4 values of individual isomers.

The magnetic field dependence of the relaxation rate constant k_r of the CS-RP is very similar for all the triad complexes investigated. An analysis is represented in some detail for complex C_{43} in Figure 6. The onset of the magnetic field dependence of the effective rate constant k_a occurs rather sharply at 3 mT and the field effect is purely monotonic. With none of the CS-RPs of the triads investigated we see what is known in the spin chemical literature as *J*-resonances and has been described for a number of linked RP systems (cf. refs 31, 34, 39, and 64). Such effects are due to T−S splittings caused by nonvanishing exchange interaction *J* and are usually observed as kinetic maxima occurring at fields $B_{max} = 2J$ where the T$_-$ or T$_+$ level (depending on the sign of *J*) crosses with the S level. Kinetic effects due to such crossings can be seen only if coherent S−T mixing processes are rate determining for the observable kinetics. In our systems this is clearly not the case because the order of 5×10^8 s^{-1} derived for k_{coh} from the $B_{1/2}$ value (cf. eq 1) is significantly faster than that observed for the apparent k_3. As we have seen in the discussion of the observed k_3 values, the electron-transfer mechanism is encounter controlled, meaning that during longer periods the two radicals are far enough apart so that no direct electron transfer does occur and also the exchange interaction should be negligibly small.

As shown in Figure 6, the rate constant k_a shows a monotonic decrease approaching a limiting value that is assigned to the direct recombination with rate constant k_4 of the T$_\pm$-CS-RP state. Like k_a the relaxation rate constant k_r evaluated according to the fitting procedure described above is a monotonic function of the field strength. Qualitatively, this is in line with the Lorentzian behavior of the longitudinal relaxation rate constant of spins given by

$$k_r = \frac{k_{r,0}}{1 + \omega^2 \tau_c^2} \qquad (13)$$

where τ_c is the characteristic correlation time and $k_{r,0}$ is the zero-field value of the relaxation rate constant. It must be remarked though, that the observed field dependence of k_r cannot be described by a relaxation process with a single correlation time. At least two components with $\tau_{c,1} \approx 0.25$ ns and $\tau_{c,2} \approx 2$ ns are needed to fit the field dependence of $k_r(B_0)$. Because the **g**-tensor anisotropy of the two radical moieties is probably small enough, relaxation mechanisms based on the *gta* mechanism and the related *src* mechanism may be neglected. Anyhow, they would be expected to show increasing values with the field (*gta*
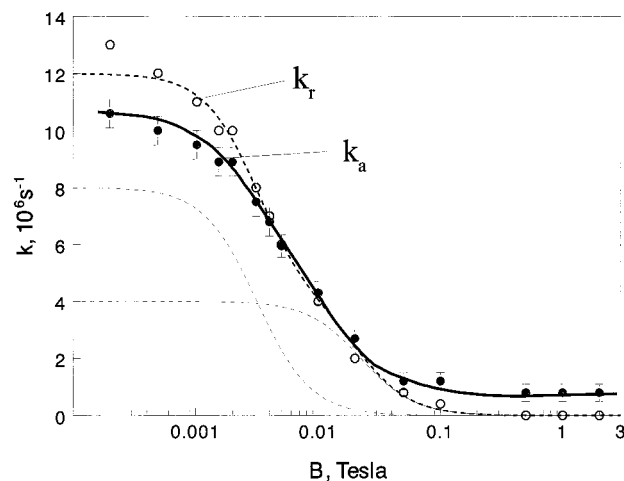

Figure 6. Magnetic field dependence of observed slow decay component k_a and relaxation rate constant k_r for triad C_{44}. The solid line through the data points for k_a (with error bars) is just drawn as a visual aid. The dashed line through the data points for k_r results from a fit using a sum of two Lorentzians, the individual curves of which are also shown (light dashed curves).

mechanism) or to be independent of it (*src* mechanism). Thus we are left with the *ahf* mechanism and the *esdi* mechanism. The stochastic modulation of electron spin dipolar interaction occurs mainly through the relative motion of the radical moieties with respect to each other, while the *ahf* mechanism depends on the individual rotational motion of the two radicals. The slower of the two approximate correlation times of ca. 2 ns, which determines the field dependence of k_r between 0.01 and 0.1 T, is quite close to what one expects for the rotational correlation time of the triad complex as a whole. This follows from the Debye equation[65]

$$\tau_r = \frac{4}{3} \frac{\pi R^3 \eta}{kT} \qquad (14)$$

with η the solvent viscosity and R the radius of the complex. Using $R \approx 15$ Å and $\eta = 0.8$ m Pa s one obtains $\tau_r \approx 2.7$ ns. The rotation of the complex as a whole will support both relaxation mechanisms *ahi* and *esdi*. The shorter correlation time of ca. 0.2 ns must be related to individual motions (rotations and relative translation changing the length and direction of the interradical distance vector) which can also support both types of relaxation mechanisms so that a more specific assignment cannot be given without detailed modeling. Nevertheless, it may be of interest that the observed relaxation behavior and absolute order of magnitude of the rate constant is very similar to that of RPs trapped in micellar supercages.[49,66] The observations regarding spin relaxation of the CS-RP indicate that the nearby Ru ion in its diamagnetic state does not affect spin relaxation of the attached radicals in a noticeable way.

While all complexes investigated yield qualitatively rather similar pictures for the set of decay curves at different fields, complex C_{41} shows a somewhat quantitatively different pattern. The high-field effects (ii.a) and (ii.b) are still comparable to those exhibited by the other complexes; however, the MFE on the decay of the slow component is much less pronounced. When analyzed in the framework of Scheme 2 the values obtained for the recombination rate constants are $k_3 = 2.5 \times 10^8$ s^{-1} and $k_4 = 3.7 \times 10^6$ s^{-1}. Both rate constants are significantly larger than for the other complexes, where k_4 ranges

(65) Debye, P. *Polar Molecules*; Dover Publications: New York, 1945.
(66) Levin, P. P.; Kuzmin, V. A. *Chem. Phys. Lett.* **1990**, *165*, 302.
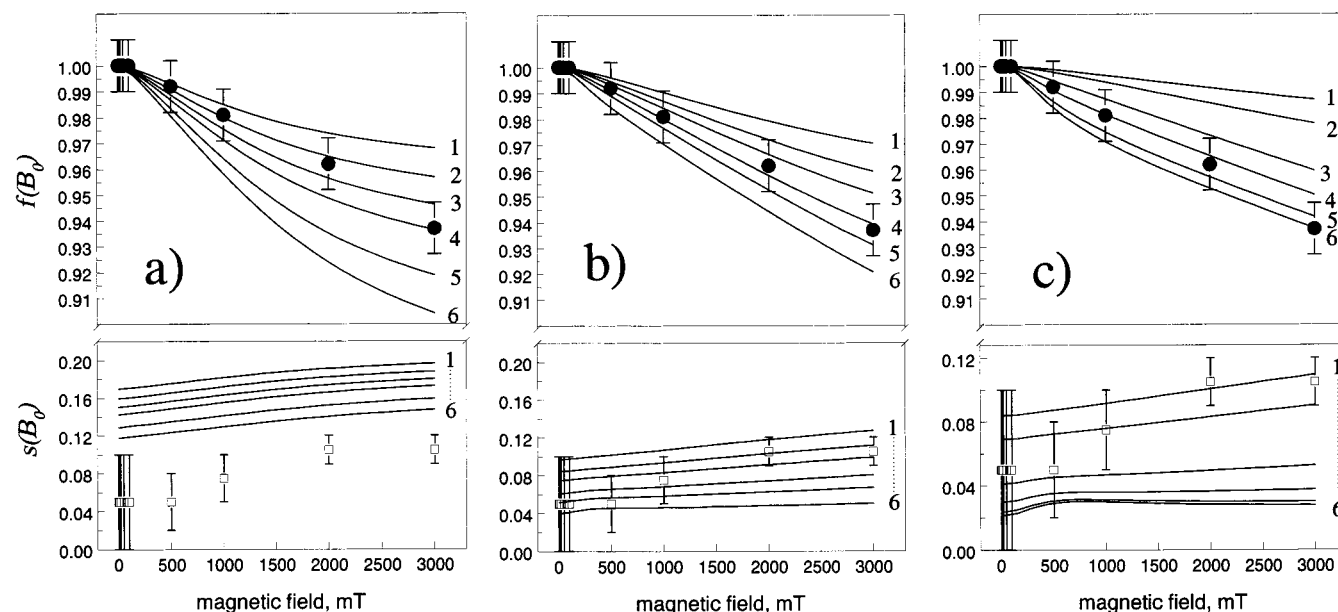
Figure 7. Magnetic field dependence $f(B_0)$ of the CS-RP amplitude and $s(B_0)$ of the initial CS-RP singlet character observed for triad C_{34} (cf. Figure 5). In panels a–c different sets of theoretical simulations are presented. For the parameters cf. Table 3.

between $(0.5$ and $1) \times 10^6$ s^{-1} and k_3 between $(0.6$ and $1) \times 10^8$ s^{-1}. The ratio of k_3/k_4 is 67 for C_{41}, which is somewhat reduced compared to those of the other complexes ranging between 100 and 150 but is still on the same order of magnitude. This supports our view that electron-transfer recombination of the CS-RP is essentially encounter dependent. The short link connecting the PTZ moiety to the complex leads to a reduction of the average separation between the DQ$^{+\bullet}$ and PTZ$^{+\bullet}$ moiety. This increases the rate of reactive encounters which has a similar effect on k_3 and on k_4. As we have pointed out above, k_4 is field independent and hence, even if the field dependence of $k_r(B_0)$ is similar to that of the other complexes, the limiting value of the slow recombination rate constant for the slow component (determined by k_4) is larger and therefore the MFE on k_a is smaller.

The value of k_3 of 2.5×10^8 s^{-1} for C_{41}, which followed from our analysis, is very close to the value of 5×10^8 s^{-1} estimated from the half-field value of the hyperfine coupling and characterizing the average rate of the nuclear spin dependent T–S mixing rate in zero field. In this case our approximation, which requires that k_3 be much faster than any spin process, becomes questionable. Now the effective recombination rate constant in zero field is rather strongly dominated by the coherent T–S mixing rate, $k_{S,To}$, rather than by $k_3/4$. Consequently, the true k_3 value is probably larger than determined in our analysis. This provides a rationale for the apparent decrease of the k_3/k_4 ratio for C_{41}. For this compound a realistic simulation of the zero- and low-field kinetics would have to resort to more sophisticated models taking explicitly into account the time dependence of hyperfine-induced T–S transitions. Such an analysis is beyond the scope of the present investigation.

(ii) The High-Field Effects. Above fields of 0.5 T when the slow part of the decay kinetics has essentially reached its high-field limit, the initial peak amplitude of the signal decreases and the relative contributions of the fast component increase at the expense of the slow component. The qualitative interpretation of these high-field effects is obvious: a decreasing amplitude indicates a decreasing yield of CS-RP formation with increasing field. On the other hand, the variation in the ratio of contributions from the fast and slowly decaying components corresponds to a change in initial spin character. A quantitative

analysis of these effects can be based on the fit parameters A_0 and s of the CS-RP decay kinetics. As mentioned above, these parameters have been evaluated in some detail for complex C_{34} (cf. Table 2 and Figure 7). They indicate a decrease of initial CS-RP yield by 6% between zero field and 3 T and an increase of the singlet character up to 9% at 3 T. As shown by the error bars in Figure 7, the s value is rather ill defined at low fields. In the field region where the biexponentially is not yet well pronounced the fitting procedure has more freedom than at higher fields. Nevertheless, when the error bars decrease at higher fields it becomes apparent that the s parameter has a tendency to increase with the field.

As pointed out in the introduction, the decrease of the CS-RP yield could be anticipated on the basis of the spin chemistry of a primary CT state involving an oxidized (Ru^{III}) complex. Hence the observed MFE represents evidence of the intermediacy of such a state. It should be noted that an alternative primary electron transfer from PTZ to the photoexcited Ru-(bpy)$_3^{2+}$, leading to a reduced complex Ru^{II}(bpy)$_2$(bpy$^{\bullet-}$)$^+$ would not give rise to a MFE of the observed kind[23] because the fast spin processes required are only exhibited with Ru in a strongly spin–orbit mixed low spin d^5 electron configuration.

The MFE on the CS-RP amplitude is completely analogous to the effect observed on the free radical yield in the photoreactions of unlinked Ru(bpy)$_3^{2+}$-type complexes with methyl viologen.[27] However, in the latter cases the subsequent decay of the observed radicals occurs by recombination in the bulk, i.e. in a non-geminate process, where spin memory is completely lost. In the present case the recombination of the CS-RP state is a geminate process and, as shown above, the kinetics of this process reveals information on the initial spin substate population in which the CS-RP is created. Thus a new type of magnetic field effect, the change of initial spin character of the CS-RP state with the magnetic field, was detectable, which would be impossible to observe with unlinked radicals.

Referring to Scheme 1, the increase of s with magnetic field can be explained as a consequence of the magnetic-field-driven ^{3}CT → ^{1}CT process. It should be noted that while this change in the spin state opens up the channel of recombination to the ground state, it does not affect the possibility of CS-RP formation which can occur equally well from ^{3}CT as from

Scheme 3
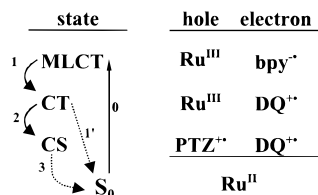
^{1}CT. Of course, due to the increased competition from channel 1′ the CS yields will be lower for ^{1}CT than for ^{3}CT but it will still be noticeable if the rate constant of process 2 (and 2′) is of comparable order of magnitude as that of process 1′. On the other hand, because of spin conservation in the electron-transfer process, the singlet character of ^{1}CT is transferred to the CS-RP created via this route. Thus the observed MFE on the parameter *s* definitely indicates a contribution of CS-RP formation that occurs subsequent to some magnetic field driven coherent ^{3}CT → ^{1}CT conversion.

For a quantitative interpretation of the high-field effects on A_0 and *s* our previously developed theory of the MFE in RPs of the Ru^{III}··MV$^{+•}$ type, which recently has been fully confirmed experimentally by picosecond time-resolved measurements,[67] may be applied to the present triad system in a straightforward manner. The process of CS-RP formation in the present triad complexes is kinetically equivalent to the cage escape process of the two unlinked Ru^{III} and MV$^{+•}$ moieties, which in our theoretical model is represented by a first-order process.[68] For the details of the theoretical model that is formulated in terms of the Stochastic Liouville equation (SLE) formalism we refer to refs 26, 31, and 69. Here we will only briefly point out the specific features distinguishing it from conventional RP theory:

The Ru^{III} moiety is formally treated as a normal spin $^1/_2$ system, but the spin−orbit mixed nature of this effective spin is consistently taken into account by the following features: (a) In a magnetic field the motion of the effective spin at Ru^{III} is described by a Zeeman Hamiltonian with the full (strongly anisotropic) **g**-tensor, and (b) there is no pure S-state in the CT-RP because the singlet character is irreducibly distributed over several of its four substates. The partial singlet characters of the substates can be obtained from the experimental **g**-tensor values of the Ru^{III} species. They are 0.85 for S′, 0.075 for T$_+$′ and T$_-$′, and 0 for T$_0$′ (cf. ref 70). (The primes are used to denote the spin−orbit mixed character of the pertinent substates.) (c) Spin relaxation of the CT-RP is governed by spin relaxation of the Ru^{III} moiety, which occurs by a rotation-independent, spin−orbit-coupling related (probably Orbach-type)[71] mechanism. It is parametrized by a single field-independent spin relaxation time $\tau_S \approx 25$ ps for both longitudinal and transversal relaxation time.[70]

In the Stochastic Liouville equation formalism spin relaxation, coherent spin motion due to the anisotropic Zeeman interaction and chemical reactions are treated consistently as simultaneous dynamic processes. From the time-integrated solution that is calculated numerically we obtain the magnetic field dependent

(67) Gilch, P.; Pöllinger-Dammer, F.; Musewald, C.; Michel-Beyerle, M. E.; Steiner, U. E. *Science* **1998**, *281*, 982.

(68) Actually this type of rate law is even more appropriate to processes 2 and 2′ in the triads than to the diffusive separation of a pair of unlinked particles.

(69) Gilch, P.; Linsenmann, M.; Haas, W.; Steiner, U. E. *Chem. Phys. Lett.* **1996**, *254*, 384.

(70) Wolff, H.-J. Untersuchungen zur Spinchemie der Photooxidation von Ruthenium(II)trisdiimin-Komplexen; Dissertation: Universität Konstanz, 1994.

(71) Kivelson, D. *J. Chem. Phys.* **1966**, *45*, 1324.

yield $\varphi_{CS}(B_0)$ of CS-RPs which may be compared to the experimentally observed field-dependent signal amplitude $A(B_0)$ of the CS-RP state. For convenience we will define the relative value:

$$f(B_0) \equiv \frac{\varphi_{CS}(B_0)}{\varphi_{CS}(0)} = \frac{A(B_0)}{A(0)} \tag{15}$$

For the present application the program has been extended to yield also the fraction of CS-RPs going into the various spin substates. This is not a trivial task since the spin chemical behavior of the CT-RP is highly anisotropic and the calculations for the CT substates are performed by using a molecule fixed basis of spin states. Therefore the resultant CS substate population has to be transformed to the laboratory frame for each of the orientations that we consider in the isotropic averaging process. The calculations give the orientational averages $p_{S,CS}$, $p_{T_0,CS}$, $2p_{T_\pm,CS}$ of the fractional yields of the CS substates. It must be noted that in a magnetic field $p_{T_0,CS}$ and $p_{T_\pm,CS}$ are not equal because of the combined effects of the difference in the reactivities of CT(T$_o$′) and CT(T$_\pm$′) and of the **g**-tensor anisotropy. Not all of the theoretically accessible substate populations are observable in our experiment. Since S and T$_0$ are in rapid equilibrium we cannot distinguish $p_{S,CS}$ and $p_{T_0,CS}$. Experimentally the parameter *s* is determined by a fit of the kinetic model for the CS-RP decay wherein it is assumed that at $t = 0$ a fraction *s* of RPs is in the singlet and a fraction $(1 - s)$ is equally distributed over the T substates. If the assumption of rapid equilibrium between S and T$_0$ is valid, in our model of the CS-RP kinetics a general initial spin state population $p_{S,CS}$, $p_{T_0,CS}$, $2p_{T_\pm,CS}$ is kinetically equivalent to a case where

$$s = (1 - 3p_{T_\pm,CS}) \tag{16}$$

We may now test the applicability of this theoretical model by comparing the theoretical results for $f(B_0)$ and $s(B_0)$ obtained by numerical solution of the SLE with the experimentally observed values. Apart from the spin-related parameters whose values have been given above we use only two adjustable kinetic parameters:

$k_{1'}$, the rate constant for recombination of the ^{1}CT-state, and $k_2 = k_{2'}$, the rate constant for the spin-independent formation of the CS state from the ^{1}CT-RP or the ^{3}CT-RP state. A comparison of theoretical and experimental results should provide both a validity check of the theoretical model and a determination of the values of the two rate constants.

Figure 7 shows an overview of typical theoretical results representing the variation of the functions $f(B_0)$ and $s(B_0)$ with k_2 and $k_{1'}$. Concerning the reasonable range of k_2, we took into account the limit of $k_2 \geq 10$ ns^{-1} that is established from direct picosecond time-resolved spectroscopy for process 2 (cf. ref 7). Figure 7a shows the results for a variation of $k_{1'}$ with k_2 fixed to 10 ns^{-1}. For a $k_{1'}$ range between 20 and 30 ns^{-1} (cf. Table 3) the theoretical curves 2−4 for the MFE characterized by the amplitude reduction factor, $f(B_0)$, approximately match the experimental points, although their curvatures are more pronounced than the experimental one. However, the pertinent theoretical $s(B_0)$ curves are significantly higher than observed. In fact, the condition to predict both $f(B_0)$ and $s(B_0)$ correctly is sufficient to fix the absolute values of k_2 and $k_{1'}$ in the model calculations. As k_2 is increased the shape of the $f(B_0)$ curves becomes less curved and gives a better match with the experimental results. Furthermore, the level of the $s(B_0)$ curves

Table 3. Rate Parameters $k_{1'}$ and k_2 and Resulting Yields φ_{CS} for the Model Calculations Shown in Figure 9[a]

curve no.	$k_2 = 10$		$k_2 = 50$		$k_2 = 100$	
	$k_{1'}$	φ_{CS}	$k_{1'}$	φ_{CS}	$k_{1'}$	φ_{CS}
1	15	0.782	50	0.888	50	0.945
2	20	0.793	75	0.852	100	0.906
3	25	0.702	**100**	**0.832**	300	0.808
4	30	0.692	**150**	**0.776**	500	0.744
5	40	0.622	200	0.740	700	0.697
6	50	0.584	300	0.683	800	0.677

[a] All rate constants are in units of ns^{-1}; parameter values yielding the best agreement with the experimental magnetic field effects $f(B_0)$ and $s(B_0)$ are printed in bold.

is decreased. In Figure 7b the series of curves with the best simultaneous fit for $f(B_0)$ and $s(B_0)$ is shown. The optimum parameter set corresponds to a value of 50 ns^{-1} for k_2 and 150 ns^{-1} for $k_{1'}$. If k_2 is chosen too high (cf. Figure 7c) the shape of the $f(B_0)$ curves is again too distorted to match all experimental points equally well. Furthermore, the level of the $s(B_0)$ curves has dropped to a too low value for $k_{1'}$ values where the $f(B_0)$ curves fit best.

We may conclude that exploitation of the $f(B_0)$ and $s(B_0)$ MFEs allows the absolute values of the two rate constants $k_{1'}$ and k_2 to be fixed with an accuracy of about $\pm 20\%$. The values thus obtained are in accord with accessory information and implications from other experiments. Thus $k_2 = 50$ ns^{-1} is in fact so much faster than $k_1 = 1.04$ ns^{-1} in triad C$_{34}$ (cf. ref 7) that the CT state is impossible to detect. On the other hand, a value of 50 ns^{-1} seems absolutely compatible with a driving force corresponding to $\Delta G_{et,2}$ of -1.35 eV[7]. The value of $k_{1'} \approx$ 150 ns^{-1} is in the same order of magnitude as values obtained from similar treatments of MFE results for free radicals in the reaction between the unlinked donors and acceptors Ru(bpy)$_3^{2+}$ and methyl viologen.[26,27,36,70]

From the theoretical calculations we also obtain a value of the efficiency φ_{CS} of CS-RP formation from the CT state. For the kinetic parameters yielding the best fit of the experimental magnetic field effects a φ_{CS} value between 0.77 and 0.83 is obtained (cf. Table 3), which compares well with the experimental value[72] of 0.86. Interestingly, the φ_{CS} value resulting from the best fit of the $f(B_0)$ curves is rather insensitive to the value chosen for k_2 (cf. Figure 7 and Table 3).

Conclusions

The present studies demonstrate how investigation of the kinetic MFEs can provide information about complex electron-transfer systems that is simply not available from traditional time-resolved methods. Photoexcitation of these triad complexes induces a cyclic sequence of electron-transfer processes comprising three types of electron-hole pair states (cf. Scheme 3). Processes 1′ and 2 are faster than process 1. However, as we have shown, their rate constants can be assessed by exploiting magnetic-field dependent spin chemical effects. Process 3 is the slowest of the electron-transfer processes, but since it is associated with rate-limiting spin processes, magnetic-field dependent measurements are required to determine the true electron-transfer rate constant.

The CS state formed in the second electron-transfer step has been shown to retain most of the triplet spin memory of the initial ^{3}MLCT state. The magnetic field dependence of the CS decay exhibits a spectacular lengthening of the lifetime of the majority (ca. 2/3) of the CS-RPs. Because the magnetic field necessary to extend the CS-RP lifetime is modest (<0.5 T) and because the effect on lifetimes is substantial (up to a factor of 10), these results should be of great interest from the stand point of photochemical energy conversion in these and related systems. In a magnetic field the decay kinetics of the CS-RP state has revealed a clear separation of the contributions of T$_\pm$ and T$_0$ components, an observation that to our knowledge has not been reported in such a distinct and quantitative way with other RP or biradical systems. The CS-RPs with the present triad systems are the first examples where the reaction scheme of the relaxation mechanism (Scheme 2) could be confirmed and exploited in full detail.

The present investigation is the first one where successive RPs of two very different types are observed in succession: the strongly spin−orbit coupled d-electron RPs and the classical organic RPs. So their different types of spin chemistry and magnetic field effects appear in conspicuous contrast.[74]

(72) This value was determined with the same laser spectrometer as used for the MFE studies. As a quantum yield reference the intensity of the ^{3}MLCT transient absorption maximum at 370 nm of the complex Ru-(DMB)$_3^{2+}$ (DMB = 4,4′-dimethylbipyridine) was used with the complex concentration adjusted so as to achieve a ground-state absorption at the laser wavelength equal to that of our sample with the triad C$_{34}$. Under the same excitation conditions the ratio of $\Delta A_{388,CS}$, the transient absorption at the maximum of the CS state spectrum of C$_{34}$, and $\Delta A_{370,ref}$, the ^{3}MLCT absorption at the spectral maximum of the reference complex, was found to be 0.54. From it the value of φ_{CS} is obtained according to the relation:

$$\varphi_{CS} = \frac{\Delta A_{388,CS}}{\Delta A_{370,ref}} \frac{\Delta\epsilon_{370,ref}}{\Delta\epsilon_{388,CS}}$$

The absorption coefficient $\Delta\epsilon_{370,ref}$ was determined as 23000 M^{-1} cm^{-1} by comparing $\Delta A_{370,ref}$ to $\Delta A_{430,ref}$ and assuming that the triplet−triplet absorption is negligible at 430 nm, so that $\Delta\epsilon_{430,ref} = -\epsilon_{430,ref}$, where $\epsilon_{430,ref} = 11000$ M^{-1} cm^{-1} is the pertinent ground state absorption coefficient of the reference complex. Since the ground state absorptions of the phenothiazine and the diquat species are negligible at 388 nm (cf. Figure 2) the value of $\Delta\epsilon_{388,CS}$ is given by[36,73] $\Delta\epsilon_{388,CS} = \epsilon_{388}(3\text{-}DQ^{+\bullet}) + \epsilon_{388}(10\text{-MePTZ}^{+\bullet}) = (13900 + 600)$ M^{-1} cm^{-1} = 14500 M^{-1} cm^{-1}. Using these values we obtain $\varphi_{CS} = 0.86 \pm 0.08\%$. It is worthy of note that this value of φ_{CS} exceeds the value reported in ref 13 by more than a factor of 3 (cf. 0.26 vs 0.86). While these two measurements were not made under identical conditions (e.g., slightly different solvent and different excitation wavelength) these differences are unlikely to be responsible for a factor of 3 difference in φ_{CS}. We suspect, therefore, that the earlier reported value of $\varphi_{CS} = 0.26$ for C$_{34}$ is in error and the correct value is much larger than previously thought.

(73) Limoges, B. R.; Elliott, C. M. Unpublished.

(74) In this regard we note that a MFE observed with Ru(bpy)$_3^{2+}$ and methylviologen in micellar solutions[75] showing the MFE characteristics of a normal organic RP might be indicative of a secondary RP being observed, formed upon conversion of Ru(III) to Ru(II) by some reducing material, e.g. the surfactant, in the system.

(75) Turro, N. J.; Khudyakov, I. V.; Gopidas, K. R. *Chem. Phys.* **1992**, *162*, 131.